



## STONE COLUMNS FOR SEISMIC GROUND IMPROVEMENT: A DESIGN AND CONSTRUCTION CASE HISTORY

### Gavin Lee

Senior Geotechnical Engineer, Amec Foster Wheeler Environment & Infrastructure, Canada  
*Gavin.t.lee@amecfw.com*

### Makram El Sabbagh

Associate Geotechnical Engineer, Amec Foster Wheeler Environment & Infrastructure, Canada  
*Makram.sabbagh@amecfw.com*

### Blair Gohl

Senior Associate Geotechnical Engineer, Amec Foster Wheeler Environment & Infrastructure, Canada  
*Blair.gohl@amecfw.com*

### Ped Zabeti

Senior Geotechnical Engineer – Team Lead, BC Hydro, Canada  
*Ped.zabeti@bchydro.com*

**ABSTRACT:** A new development project in the Fraser Valley Regional District in British Columbia involved the construction of a new electrical substation. The substation is located on sloping terrain in a seismically active area. Ground conditions at the site consist of an upper layer of non-engineered soft fills extending to depths of 15 m in some areas, which are underlain by generally stiff low to medium plasticity silt with frequent interbedded lenses of low to non-plastic sandy silt/silty sand. Based on the results from the site investigations programs, these lenses were considered to be horizontally continuous throughout the site. Given the inferred relative density in the low to non-plastic sandy silt/silty sand lenses and considering the 2% in 50-year recurrence interval design seismic event, liquefaction triggering was anticipated in those lenses, which would result in large seismic and post-seismic movements and possibly lead to slope failures. Ground improvement using bottom feed vibro-replacement (stone columns) was adopted to reinforce the ground, therefore preventing slope failure and keeping the seismically induced movements to within acceptable limits. Over a thousand stone columns were constructed in a triangular pattern to a depth of 25 m with an average diameter of 1.13 m, resulting in an area replacement ratio of 16%. This paper presents the results of the stability evaluations and dynamic finite element modeling that was conducted to assess the seismically induced movements, as well as the methodology adopted in the design of the stone columns. Some of the challenges encountered during stone column construction are presented and discussed, including the occurrence of large sand boils in the lowland area of the site.

### 1. Introduction and Background

A new substation was to be constructed to assist with new developments in the Fraser Valley Regional District in British Columbia, Canada. The new substation is located on sloping terrain and would consist of two multi-level buildings housing one 60 kV Gas Insulated Switchgear (GIS) and one 25 kV GIS Feeder section with attached reactor bays, one single story Control Building, switchyard structure, transformers, capacitor bank, and associated parking areas and access roads. Ground conditions at the site consisted of a large amount of loosely placed non-engineered fills up to 15 m thick underlain by native materials that were deemed to be susceptible to liquefaction during a design seismic event (2% in 50-year probability of exceedance design earthquake event). Native materials consisted of generally stiff low to medium plasticity silt with frequent interbedded lenses of low to non-plastic sandy silt/silty sand.

Liquefaction under seismic shaking is defined as the temporary loss of strength of loose to compact saturated cohesionless or low plastic cohesive soils due to build-up of excess pore pressures under cyclic loading. Liquefaction was deemed to be a concern in the interbedded lenses of low to non-plastic silty sand and sandy silt, which were observed within the native low to medium plasticity silt matrix at the site.

The existing site conditions (prior to site preparation works) consisted of an upper area with a surface elevation varying between +20 m to +24 m approximately, and a lower area with elevations around +15 m. The property is bounded to the southeast and southwest by an avenue, to the east and to the northwest by two streets, and an adjacent property to the northeast. The avenue, which borders the site towards the south, is at an elevation of about +8.5 m. Existing slopes on site varied from steeper than 1H:1V at the southwest, to 3H:1V or milder to the east, west and north.

Key design issues for this project were to minimize post-seismic differential movements across or between structures and minimize the effects of these differential movements on cabling or transformer overhead lines entering the facility. Since the facility would be located at the top of a slope, minimizing post-seismic differential movements would largely be governed by slope stability considerations and the influence of soil liquefaction within the slope.

## 2. Site Description

### 2.1. Structure Layout and Loading Conditions

The new substation would consist primarily of two multi-level buildings and the general layout of the structures is shown on Fig. 1. It was decided that the substation would be placed at an elevation of about +18.5 m in order to try to optimize and balance excavation cut and fill volumes. The building and structure loads generally varied between 50 kPa to 100 kPa.



Fig. 1 – Substation Layout Plan

### 2.2. Subsurface Conditions at the Site

The site is located at the border line of post-glacial quaternary deposits and Pleistocene Sumas Drift based on the British Columbia Geologic Survey map. The subsurface conditions at the site were observed to generally consist of an upper fill layer that is up to 15 m thick and approximately up to 10 m thick under the northern corners of the substation structures. The fill is heterogeneous, ranging from low to medium plasticity silt or clayey silt to loose silty sand with gravel and occasional cobbles. Organic

materials were also noted in the fill containing roots, logs, wood chips, and fibers. Standard Penetration Test (SPT) blowcounts in the fill varied between 0 and 8 blows per 0.3 m, and an average blowcount of approximately 4 blows per 0.3 m.

The fill is locally underlain by organic peat. The thickness of the peat/organic silt generally varies between 0.3 m and 0.5 m. The fill and peat layers are generally underlain by a stiff, low to medium plasticity silt, except in the area east of the substation and some other localized areas where the silt is believed to be firm. The consistency of the native silt generally ranges from firm to becoming stiff to very stiff with increasing depth. The Plasticity Index (PI) of the native silt generally varies between 5 and 20. However, low plasticity silty sand lenses were encountered within the silt matrix having PI values less than 5. The silty sand/sandy silt interlayers were generally below elevation +12 m, which are considered to be potentially liquefiable under design levels of seismic shaking and play an important role in the seismic response of the slopes around the substation site. Fines content in the silty sand/sandy silt interlayers generally varies between 30% and 60%.

SPT blowcounts in the silt generally vary between 5 and 9 between elevations +13 m to +20 m and generally increase to between 10 to 20 below elevation +10 m. Based on interpretation of cone penetration testing (CPT) and undrained strength values measured using a Nilcon field vane, a design undrained strength distribution with depth was selected for the native silt. The undrained shear strength was determined to be about 50 kPa increasing linearly with depth at 3 kPa per meter. The Overconsolidation Ratio (OCR) used in the design was estimated to be in the order of about 1.3 to 2.0. However, based on one-dimensional consolidation tests and field vane tests the OCR could be higher. It was anticipated that the native silt could have an OCR in the range of 3.5 to 6.0. The silt matrix is considered to have a low susceptibility to liquefaction due to the high OCR and low to medium plasticity.

The interbedded lenses of low to non-plastic silty sand and sandy silt that were observed within the low to medium plasticity silt matrix were observed to be about 25% of the total thickness of the native silt and were typically close to being continuous throughout the site. The thicknesses of these lenses were generally less than 0.5 m, although thicker lenses (up to 0.7 m) were observed. CPT data indicated  $q_{c1,ecs}$  (normalized overburden and equivalent clean-sand corrected cone tip resistance) values of between 5 MPa to 12.5 MPa for the lenses.

Water level readings taken from standpipe piezometers installed at the site revealed a water table at elevations between +9.5 m to +18 m. The water level measurements suggested the existence of perched water levels.

### 3. Liquefaction Evaluation

Liquefaction triggering evaluations based on both laboratory testing and CPT were completed to determine the liquefaction susceptibility of the native soils.

The natural moisture contents ( $w_n$ ) of the silty sand and sandy silt lenses were tested and were generally greater than their corresponding Liquid Limit (LL) values, with the ratio of  $w_n/LL$  typically varying between 1.0 and 1.4 and having a PI less than 5. This indicates that the lenses would likely be subject to cyclic pore pressure generation based on criteria provided by Bray and Sancio (2006).

CPT based liquefaction triggering evaluations were performed following the procedure proposed by Idriss and Boulanger (2008). The capacity of a soil to resist cyclic pore pressure generation and liquefaction is generally expressed in terms of the Cyclic Resistance Ratio (CRR). CRR is directly related to the in-situ density, degree of over-consolidation and fines content characteristics of the soil as well as confining stress levels and initial static shear stresses at the depth of interest. The analysis uses the cone tip resistance ( $q_c$ ) and sleeve friction ( $f_s$ ) to determine the CRR in conjunction with the estimated Cyclic Shear Stress Ratios (CSR) versus depth that are likely to develop at the site in the event of the design earthquake. The effective CSR was calculated using one dimensional and two dimensional dynamic site response analysis. Selection of input earthquake motions applied at "firm ground" level (i.e. Site Class C soils as defined in the 2010 National Building Code of Canada (NBCC)) were made consistent with 2010 NBCC ground motion levels and using ground motion time histories recorded during California earthquakes having magnitudes (M) in the range of M6.1 to M7.1. Firm ground level was considered to be in the order of elevation -25 m based on shear wave velocity measurements completed onsite. The records were filtered to approximately match the target Site Class C elastic response spectrum given for

the site in the 2010 NBCC. Results from the analyses indicated that liquefaction triggering (high cyclic pore pressure generation due to seismic shaking) would likely occur in the thinner sandier lenses rather than in the stiffer silt matrix outside the lenses.

Stress-controlled cyclic  $K_0$ -consolidated direct simple shear (DSS) tests were performed on samples of sandy silt under constant volume conditions and each test specimen was consolidated to an effective vertical consolidation stress of 250 kPa. The degree of saturation of the samples after consolidation generally ranged from between 90% to 100%. Stress levels were selected to be representative of the average effective vertical stress along a typical critical failure plane determined from limit equilibrium slope stability models. Results of the cyclic DSS tests on samples of the silty sand/sandy silt lenses indicate CRR values in the range of 0.20 to 0.25 for around 12 stress cycles, which is considered to be representative of the number of effective shaking cycles for a magnitude 7.0 design earthquake. Large excess cyclic pore pressures ( $R_u$  close to 100%) were generated when the samples were subjected to CSR values equivalent to the above CRR values. The laboratory CRR values compare generally well with the CPT based CRR values processed using the Idriss and Boulanger (2008) method, which indicate CRR values typically in the range of 0.2 and in some cases higher.

Post-cyclic DSS tests indicate residual strength ratios ( $S_r/\sigma'_{vo}$ ) in the order of about 0.2. These measurements are for constant volume conditions and neglect the effects of pore pressure redistribution, water layer formation and possible volumetric expansion that could occur in these silty sand lenses following earthquake shaking. Therefore the residual strength ratios could be lower (about 0.1) based on recommendations provided by Idriss and Boulanger (2008).

#### **4. Stability Analyses**

Limit equilibrium stability evaluations were performed using the post-liquefied strength parameters in the native silt containing the interbedded liquefiable silty sand lenses. A residual strength ratio ( $S_r/\sigma'_{vo}$ ) of 0.1 was used to characterize the undrained shear strength in the native silt with the liquefied lenses. Where there is limited continuity between lenses, then the use of this  $S_r/\sigma'_{vo}$  was judged to be conservative. The slope stability model therefore included the intact undrained strength of the clayey silt between the liquefiable lenses modeled with interbedded liquefiable silty sand/sandy silt lenses that were each 1 m thick in between a 3 m thick silt matrix.

Results of the limit equilibrium model indicated a factor of safety (FS) in the order of 0.9 in absence of ground improvement. The relatively low post-seismic FS value implies that relatively large lateral ground deformations and post-liquefaction settlements should be expected following the design earthquake, which would affect building foundations in the substation. Maximum horizontal movements during shaking and at the end of shaking at the crest of the slope would need to be limited to less than 350 mm and post-seismic foundation settlements (excluding volumetric reconsolidation) to be in the order of less than 300 mm. Ground improvement was therefore required to reduce the impact of slope deformations on the post-seismic performance of the substation structures.

Evaluation of the seismic deformation potential was carried out in more detail using two dimensional finite element modeling using dynamic effective stress analysis. The finite element modeling considered cyclic pore pressure generation in the liquefiable silty sand lenses. Two dimensional dynamic response analyses of a typical slope section were performed using the plane-strain finite-element based computer program VERSAT-D2D (Wutec Geotechnical International, Version 2011.04). The model considers the effects of cyclic pore pressure generation in the silty sand lenses which leads to progressive stiffness and strength reduction in the soil elements. Dynamic total stress analysis was also carried out (i.e. with no pore pressure generation considered) to calculate CSR values for use in liquefaction triggering evaluations. The calibration of pore pressure generation models in the lenses were based on the results from laboratory cyclic DSS testing and CRR values inferred from CPT data using the methods of Idriss and Boulanger (2008). Results indicate that ground improvement would be necessary in order to keep maximum horizontal movements at the crest of the slope to less than 350 mm during the seismic event.

#### **5. Ground Improvement Design**

Based on the stability analyses and dynamic modeling, it was determined that a 35 m wide zone of ground improvement to a depth of 25 m using vibro-replacement (stone columns) would be required to reinforce the slopes. A stone column area replacement ratio (ARR) of 16% was deemed required in order

to meet the post-seismic slope stability criteria of a FS of about 1.2 and keep to a minimum the seismically induced ground deformations. The stone columns were intended to reinforce the ground and provide drainage following seismic shaking. The process of stone column installation was assumed not to cause significant densification in the sandy silt/silty sand lenses, and that liquefaction would therefore still occur in the lenses between the stone columns. The equivalent friction angles for the stone column reinforced ground were calculated based on the ARR of the stone columns (using a triangular grid and a center-to-center column spacing of 2.5 m) assuming a 42 degree friction angle in the gravel column and an effective friction angle of 6 degrees (inverse tangent of 0.1) in the assumed liquefied silty sand lenses. The method of equivalent friction angle calculation is described by Greenwood and Kirsch (1983). A total stone column ground improvement area of approximately 6,400 m<sup>2</sup> was deemed necessary, as shown shaded in grey on Fig. 2.

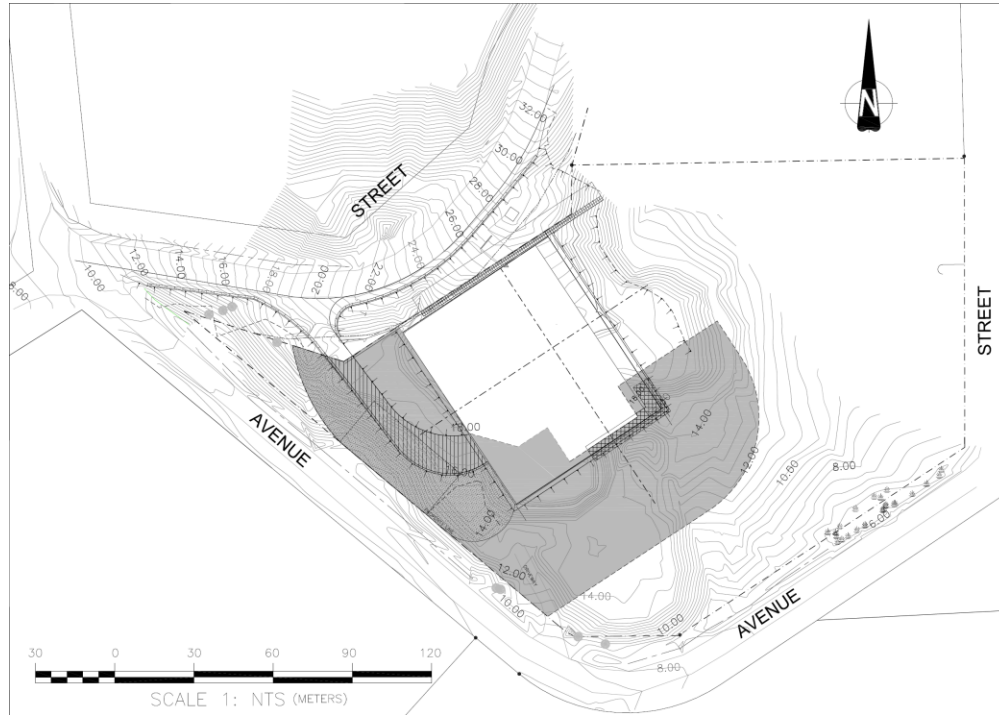


**Fig. 2 – Stone Column Ground Improvement Plan**

The ground improvement area was modeled in VERSAT-D2D to determine seismic deformations and the maximum horizontal movements during shaking and at the end of shaking were 350 mm and 300 mm, respectively, at the crest of the slope considering a stone column spacing of 2.5 m. Those lateral movements occur in the downslope direction and attenuate with distance away from the crest of the slope. Differential lateral movements of up to 100 mm are anticipated to occur over a distance of 15 m approximately, which corresponds to a “pull apart ratio” of 1/150 approximately. Those post-seismic deformations were deemed acceptable for the substation.

Post-liquefaction volumetric reconsolidation is also expected to take place as cyclically generated excess pore pressures are dissipated by expulsion of water. The methodology presented by Seed et al. (2003) was considered in the evaluation of the volumetric reconsolidation. Post-seismic foundation volumetric reconsolidation settlements are anticipated to be in the order of 500 mm considering movements occurring immediately following the end of design earthquake shaking and longer term. Structural mat foundations tilt of up to 1/50 is to be anticipated, in addition to an angular distortion in the order of 1/50 within the flexible foundations system. As a result, upper bound differential settlements within a flexible mat foundation system could be up to 4% (1/25) of the distance between column supports. Ground improvement underneath the structures could be used to further limit the differential movements. However, the differential movements were deemed to be acceptable for the structures, which generally consisted of rigid block foundations designed to tolerate the movements.

## **6. Stone Column Construction**

Ground improvement (stone column installation) works at the site were conducted over a six-month period in 2013. A stone column test section was initially conducted to assist the ground improvement contractor in determining and optimizing the stone column installation procedure to meet the required design and project specifications.

### **6.1. Methodology**

Vibro-replacement (stone columns) installation was carried out using bottom feed methods. In the bottom feed process, an electrically driven 375 mm diameter vibrator (or vibroflot) suspended by a crane penetrates to the design depth of 25 m by means of the vibrator's weight and vibrations. The crushed stone is initially loaded into a skip bucket, which is used to convey the aggregate to the hopper located at the top of the feed pipe. The stone is then fed to the vibrator tip through a 200 mm diameter feed pipe attached to the vibrator and fills the void created as the vibrator is lifted a few meters above the starting depth. The vibrator is then lowered, densifying and displacing the underlying stone to create a stone column with the desired diameter. The vibro-replacement process is repeated until a stone column is constructed to the ground surface. The experience of the vibro-replacement operator is critical in ensuring that the diameter and uniformity of the stone column are achieved. This bottom feed vibro-replacement method creates a continuous dense stone column with a somewhat uniform diameter, which reinforces the treated ground by providing additional shear strength and drainage during and following a major seismic event.

Full-time field monitoring was provided by the design geotechnical engineers during stone column installation. Field staff monitored volumes of crushed rock installed (from which ARR was estimated), amperage draw from the rig vibrator, and methodology used to ensure that stone column installation was completed in a satisfactory manner as well as in accordance with the project specifications and the design intent.

### **6.2. Test Section**

Prior to the installation of stone columns in the production area, a test section consisting of ten stone columns was installed in an area adjacent to the production area on the southern corner of the site.

The purpose of the test section was to assist the ground improvement contractor in the selection of the stone column diameter to meet the mandated ARR of 16%, ensure the proposed column spacing is achievable with the equipment mobilized to site, and generally optimize the stone column installation procedure.

In order to achieve the specified ARR of 16%, a stone column diameter of approximately 1.13 m was adopted by the contractor, with stone columns installed in a triangular pattern and a center-to-center spacing of 2.5 m.

CPTs were completed pre and post stone column installation in the test section to observe if there were any notable changes in the cone tip resistance achieved in the silty sand lenses. Results indicated generally limited improvement in the CPT tip resistance, although increases of up to 40% were occasionally noted in some instances. The results however do not preclude the triggering of liquefaction considering the design seismic event and hence a reinforcement strategy was selected as the optimal method to confirm that project specifications were achieved.

#### **6.2.1. General**

Stone columns were generally installed on two benches at approximate elevations +14 m and +17 m, with the exception of the area underlying a reinforced access road slope at the southwestern portion of the site where the working surface was as low as elevation +9 m. A total of 1,024 stone columns were installed in the field, including six deficient columns and four replacement columns.

Production stone column installation progressed for six months using two rigs and the same methodology as during the installation of the test section. Production was stopped for several days as a result of the sand boil activities during stone column installation. The sand boils are discussed further in section 6.2.4.

### 6.2.2. Area Replacement Ratio

Stone columns were installed in a triangular grid at a center-to-center spacing of 2.5 m and to a depth of 25 m. The evaluation of the in-situ stone column diameter was based on the following considerations:

- One skip bucket filled with crushed rock that has a volume of  $1.83 \text{ m}^3$  approximately was used to install a stone column interval of 1.37 m (4.5 feet);
- The amount of crushed gravel remaining in the skip bucket after it was emptied in the hopper typically varied between of  $0.1 \text{ m}^3$  and  $0.2 \text{ m}^3$  based on measurements made by the design engineers during the course of column installation. Therefore  $0.15 \text{ m}^3$  were considered in the ARR evaluation;
- A crushed rock volume that varied between around half a skip bucket to slightly over one full skip bucket was estimated to be wasted during a typical stone column installation. Therefore a volume of one full skip bucket (or  $1.83 \text{ m}^3$ ) was considered to be wasted during a typical stone column installation;
- The minimum and maximum void ratios in the crushed rock were estimated to be around 0.2 and 0.5, respectively, based on results from laboratory testing as well as information available in the literature (Fang (1991) and USBR (1998)). The relative density of the crushed rock loaded in the skip bucket was assumed to be in the order of 20%, and around 80% when compacted in the as-built stone columns. For these parameters, the corresponding decrease in volumetric strain of the crushed rock material from the time it is loaded in the skip bucket to the time it is placed in the ground is 12.5%.

Using the considerations above, the actual in-situ volume of the crushed rock that would correspond to a 1.37 m long section of stone column is  $1.41 \text{ m}^3$ , which corresponds to an in-situ stone column cross-sectional area of  $1.029 \text{ m}^2$  and a corresponding diameter of about 1.14 m. Given that the total number of stone columns that were installed and which were deemed to meet the project specifications is 1,018, the total effective stone column surface area was  $1,048 \text{ m}^2$ , which is approximately 0.164 times of the total ground improvement surface area ( $6,400 \text{ m}^2$ ), shown in grey on Fig. 2. Therefore the as-built stone column ARR on the project was on the order of 16.4%, which meets the specified minimum of 16%.

### 6.2.3. Issues Encountered

The large majority of the stone columns were installed in accordance with the design intent and specifications. Various issues prevented some of the columns (approximately 3.5% of the total number of columns) from being installed in strict agreement with the specifications such as refusal prior to reaching the design depth and smaller column diameters due to the presence of dense soil layers. In summary, the total acceptable stone columns that were installed is 1,018, with an additional six stone columns deemed to not have met the design intent.

### 6.2.4. Sand Boils

As a result of the stone column installations, several sand boils developed at the toe of the slope around the southern edge of the site (along the avenue). Consisting of discrete points where water and soil discharged from the ground during installation activities, sand boils first developed during installation of the test section and were subsequently noted during stone column production, in particular at locations close to the crest of an existing slope (sand boil #1). Sand boils are believed to be the result of the large air pressures used at the tip of the vibroflot during initial penetration as well as during construction of the stone columns, which were typically in the order of 600 kPa to 700 kPa. Such pressures are notably higher than the overburden soil pressures in the upper 25 m, thereby causing “fracturing” of the ground and resulting in such boils.

Up to approximately  $3 \text{ m}^3$  of sand and silt were ejected during the installation of any individual column, although the ejected volumes were typically less than  $0.5 \text{ m}^3$ . In general, ejection of sand and silt from sand boils exceeding  $0.1 \text{ m}^3$  per column occurred in about 16% of the stone columns only, with volumes exceeding  $0.5 \text{ m}^3$  occurring in less than 2% of the columns. Only three columns resulted in sand and silt volumes ejected from sand boils exceeding  $1 \text{ m}^3$ .

By the completion of stone column installation, 11 sand boil locations had developed, primarily aligned along the southwestern edge of the site.

With the exception of sand boil #1, the diameter of the sand boils typically varied between 0.5 m and 1 m approximately. The diameter of sand boil #1 reached 3 m approximately, during the installation of a column that resulted in the ejected approximately 3 m<sup>3</sup> of sand and silt. Photos of a sand boil are shown on Fig. 3.



**Fig. 3 – Sand boil**

Sand boil material was regularly cleaned using a hydro-vacuum truck, as directed by the project's environmental monitor. This was required in order to avoid downstream fish impact from sediment leaching deposition.

In addition to environmental concerns, sand boil activity raised geotechnical concerns regarding the stability of slopes under static conditions. Subsurface voids or areas of softened silts could result from the sand boil activity, which would lead to stability concerns in the event that such anomalies were to be aligned along a potential failure surface. An extensive program of post-densification CPT testing was adopted to verify that any soft zones or voids created during stone column installation did not impact the long-term stability of the reinforced ground at the site. One subsurface void between elevations +1.7 m to +1.9 m and several softened zones were noted within the native plastic silt during the post-densification CPT testing program.

It was noted by the design engineer's field monitors that column installation sequencing appeared to have the greatest effect on the magnitude of sand boil discharge. Through discussions with the general contractor and ground improvement contractor, an installation sequence that consisted of installing first the outermost two rows of stone columns closest to the slope was developed. This recommendation was followed on the southeastern side of the production area, and very limited sand boil activity occurred in that area once the recommendation was followed. However, the recommended sequence was not followed by the contractor on the southwestern edge of the production area, where the majority of the sand boils occurred.

### **6.3. In-Situ Testing**

To check the effectiveness of the densification works, CPTs were performed periodically after the stone column installation was completed in a given area. In total, 36 post-densification CPTs were performed in the stone column production area.

Post-densification CPT tip resistance values indicated that some limited level of densification was noted in the liquefiable lenses following the stone column installation, with increases in CPT tip resistances typically on the order of 10% to 30%. However, the CPT values were well below those required to prevent the onset of liquefaction based on standard correlations between corrected cone tip resistance and cyclic liquefaction resistance. Some reductions in undrained strength were locally observed in the plastic silts following the installation of the stone columns and are believed to be due to the disturbance



involved during the vibro-replacement process resulting in soft soil zones. However, it should be noted that some level of strength gain over time was noted in the plastic silts with long-term undrained strength profiles exceeding or returning to the design strength profile in most areas. It is believed that the strength increase noted is the result of positive excess pore pressure dissipation in the plastic silts, which were generated as a result of the large lateral stresses in the soils arising from the stone column installation process.

#### **6.4. Slope Stability Analyses**

In order to determine the effect of the softer soil zones on the overall stability of the slopes, sections were analyzed with and without soft soil zones introduced into the soil mass. Limit equilibrium stability evaluations of various case scenarios were conducted with soft lenses to reflect the area of the soft zone encountered from the CPTs. The soft lenses were generally 1 m to 2 m thick and the soft zones were assumed to vary extending from the half width of the stone column zone (17.5 m) to worst cases where the soft zones were the full width of the stone column zone (35 m). The undrained shear strength of the soft lenses generally varied from between 25 kPa to 50 kPa based on interpretations from the CPTs. An equivalent friction angle and cohesion were used to model the strength of the stone column ground improvement zone.

The FS for both the soft lenses extending the half widths and full widths of the stone column zone were greater than 1.5. These results indicate that the ground improvement strengthening of the underlying soils and the soft soil zones due to their depth and geometry did not greatly affect the overall stability of the slopes.

Post-seismic stability scenarios were also conducted with the soft lenses extending both the half and full widths of the stone column zone and laterally continuous and horizontal 1 m thick liquefiable silty sand and sandy silt lenses vertically spaced at 4 m. A  $S_r/\sigma'_{vo}$  of 0.1 similar to the previous post-seismic limit equilibrium stability and VERSAT-D2D modelling was used to characterize the undrained shear strength in the liquefied lenses. Results indicate a FS greater than 1.3 for the post-seismic stability cases.

#### **7. Drainage blanket**

As a requirement following the completion of the ground improvement, a stone column drainage blanket with a minimum thickness of 0.5 m and having a hydraulic conductivity in the order of  $10^{-1}$  to  $10^{-2}$  m/s was required to be placed in the areas where the stone columns were installed. This drainage blanket was needed at the top of the stone columns to hydraulically connect the columns to the drainage blanket and to enable drainage of excess pore pressures following the design earthquake. It was critical that the hydraulic connection be properly constructed to ensure that the stone columns function as designed and intended to meet design requirements. It was therefore recommended that the upper material on top of the stone columns be completely removed to expose the clean crushed stone column material. This upper layer has a high fines content due to the stone column construction and was usually in the order of 1 m thick, but could be thicker in some areas.

The stone column drainage blanket was required to be installed at all stone column ground improvement areas with a few exceptions where there was already free draining material above the columns. A non-woven geotextile would also be needed between the drainage blanket and overlying fills or topsoil to prevent fines from washing into the drainage blanket.

A 5 m wide section (measured horizontally in plan) running along the entire southern portion of the ground improvement area (which is approximately 250 m long, excluding the southwestern reinforced slope area that is approximately 35 m long) was also required to be fully exposed without any fill/topsoil cover on top of the drainage blanket. This would allow the drainage blanket to drain freely after an earthquake.

#### **8. Conclusion**

Based on the site investigations and engineering evaluations, the interbedded lenses of low to non-plastic silty sand/sandy silt observed within the native low to medium plasticity silt matrix is susceptible to liquefaction. Analyses indicated that lateral and vertical seismic movements at the locations of the substation structures at the top of the slope would be magnified by the presence of the sloping terrain. It was recommended that ground improvement using stone columns be completed under the slopes to

improve post-seismic stability of the slopes and to reduce seismically-induced movements of the substation structures. During the stone column installation sand boils were noted in the lower elevation areas to the south of the site. The sand boils were believed to be the result of the large air pressures used at the tip of the vibroflot during construction of the stone columns and such pressures were notably higher than the overburden soil pressures in the upper 25 m. The latter could have caused ground fracturing, which is believed to be the main reason behind the sand boils. Discussions with the ground improvement contractor after these sand boil effects were observed indicated very little prior experience with this occurrence during bottom feed methods of vibro-replacement.

It was noted that the stone column installation sequencing appeared to have the greatest effect on the occurrence and magnitude of sand boil discharge. In order to limit the incidence of sand boils, an installation sequence that consisted of installing first the outermost two rows of stone columns closest to the slope was developed. This recommendation was followed on the southeastern side of the production area and resulted in very limited sand boil activity occurring in that area. However, the recommended sequence was not followed on the southwestern edge of the production area, which is where the majority of the sand boils occurred. It was observed that the sequencing of stone columns can play an important role in limiting the occurrence of sand boils.

Based on the CPTs completed post-stone column installation, some densification was noted in the liquefiable lenses following the stone column installation, with CPT tip resistances following stone column installation typically 10% to 30% higher. However, the post-densification CPT tip resistance values were still well below those required to prevent the onset of liquefaction based on standard correlations between corrected cone tip resistance and cyclic liquefaction resistance. This is consistent with the design basis that relies on the stone columns to reinforce the ground but assumes that seismic liquefaction could occur between stone columns during a major seismic event. As a result, a stone column replacement ratio of 16% was required to ensure the site stability and limit the ensuing total and differential movements during and following the design earthquake event. The stone column ground improvement was completed successfully and the substation and associated structures were constructed at the site.

## 9. References

- BRAY, J.D., SANCIO, R.B., "Assessment of the Liquefaction Susceptibility of Fine-Grained Soils", *Journal of Geotechnical and Geoenvironmental Engineering*, Vol. 132, No. 9, September 2006, pp. 1165-1177.
- GREENWOOD, D.A., KIRSCH, K., "Specialist Ground Treatment by Vibratory and Dynamic Methods", *Piling and Ground Treatment*, Institution of Civil Engineers, March 1983.
- IDRISS, I.M., BOULANGER, R.W., *Soil Liquefaction During Earthquakes*, Earthquake Engineering Research Institute, MNO-12, 2008.
- SEED, R.B. et al., "Recent Advances in Soil Liquefaction Engineering: A Unified and Consistent Framework", *26<sup>th</sup> Annual ASCE Los Angeles Geotechnical Spring Seminar*, Keynote Presentation, H.M.S Queen Mary, Long Beach, California, April 2003.
- FANG, H.Y., *Foundation Engineering Handbook*, Chapman & Hall, Ed. 2, 1991.
- U.S. DEPARTMENT OF THE INTERIOR BUREAU OF RECLAMATION, *Earth Manual, Part 1*, Ed. 3, 1998.